PUBLICATIONS OF THE ASTRONOMICAL SOCIETY OF THE PACIFIC, **117**:256–261, 2005 March

Color and Metallicity Distributions of M81 Globular Clusters

JUN MA, XU ZHOU, JIANSHENG CHEN, ZHENYU WU, YANBIN YANG, ZHAOJI JIANG, AND JIANGHUA WU

National Astronomical Observatories, Chinese Academy of Sciences, Beijing 100012, China; majun@vega.bac.pku.edu.cn

Received 2004 November 30; accepted 2004 December 17; published 2005 March 3

ABSTRACT. In this paper we present catalogs of photometric and spectroscopic data for globular clusters (GCs) in M81. The catalogs include *B*- and *V*-band photometric and reddening data of 95 GCs, in addition to spectroscopic metallicities of 40 GCs. Using these data, we make some statistical correlations. The results show that the distributions of intrinsic *B* and *V* colors and metallicities are bimodal, with metallicity peaks at [Fe/H] ≈ -1.45 and -0.53, respectively, as has been demonstrated for our Milky Way and M31. The relation between spectroscopic metallicity and intrinsic *B* and *V* color also exists as it does for the Milky Way and M31.

1. INTRODUCTION

Great progress has been made in the past decade in our understanding of globular cluster systems of galaxies, especially the discovery that many galaxies possess two or more distinct subpopulations of globular clusters (GCs; e.g., West et al. 2004 and references therein). GCs are fossils of the earliest stages of galaxy formation and are groups of stellar populations with a single age and metallicity. Consequently, their integrated properties, such as abundance and kinematics, can provide us with valuable information about the nature and duration of the formation of their parent galaxies (Barmby et al. 2000). The metallicity distribution of GCs is of particular importance in deepening our knowledge of the dynamical and chemical evolution of the parent galaxies. For example, the GCs of many elliptical galaxies show multimodal metallicity distributions, suggesting that multiple star formation episodes occurred in these elliptical galaxies in the past (Zepf & Ashman 1993; Barmby et al. 2000).

Côté (1999) presents a metallicity distribution of 133 Galactic GCs that apparently shows two peaks (i.e., two distinct metal-poor and metal-rich GC populations). The double-Gaussian can best fit these two subpopulations; the mean metallicity values are -1.59 and -0.55 dex, respectively. Using the data for 247 GCs in M31, Barmby et al. (2000) studied the metallicity distribution, which is asymmetric, implying the possibility of bimodality. Then the applied KMM algorithm showed that the metallicity distribution is really bimodal. Perrett et al. (2002) confirmed the conclusions of Barmby et al. (2000).

M81 is the nearest large spiral outside the Local Group, and its GCs are an important target of study. However, to date, there are only a few papers that have studied the GCs in M81. The main reason is that at the distance of M81, the diameters of GCs are typically comparable to the seeing disk, and it is difficult to recognize GCs on the basis of image structure from ground-based observations, except at sites with exceptionally good seeing. To maximize the success rate of the GC candidate list for the ongoing spectroscopic observations, Perelmuter & Racine (1995) used an extensive database that included photometric, astrometric, and morphological information on 3774 objects covering a $>50'$ diameter field centered on M81 to reveal 70 GC candidates within a 11 kpc galactocentric radius. Perelmuter et al. (1995) then confirmed 25 bona fide M81 GCs from the spectroscopy of 82 bright GC candidates in the M81 field. Schroder et al. (2002) presented moderate-resolution spectroscopy for 16 GC candidates from the list in Perelmuter & Racine (1995) and confirmed these 16 candidates as bona fide GCs. They also obtained metallicities for 15 of the 16 GCs. With the superior resolution of the *Hubble Space Telescope* (*HST*), M81 is close enough for its clusters to be easily resolved on the basis of image structure (Chandar et al. 2001). Thus, using the *B*, *V*, and *I* bands of the *HST* Wide Field Planetary Camera 2 (WFPC2), Chandar et al. (2001) imaged eight fields covering a total area of ~40 arcmin^2. They reported 114 compact star clusters in M81, 59 of which are GCs.

The outline of the paper is as follows. Details on the collection of GC data are given in § 2. In § 3 we provide some statistical relationships. The summary and discussion are presented in § 4.

2. A CATALOG OF PHOTOMETRIC DATA OF GLOBULAR CLUSTERS

2.1. Sample of Globular Clusters

The sample of GCs in M81 presented here is from Perelmuter et al. (1995), Schroder et al. (2002), and Chandar et al. (2001). Perelmuter et al. (1995) obtained spectra for 82 bright GC candidates in the M81 field and confirmed 25 bona fide GCs. Schroder et al. (2002) observed moderate-resolution spectroscopy of 16 GC candidates selected from the candidate list of Perelmuter & Racine (1995) and confirmed all as bona fide GCs. Chandar et al. (2001) discovered 114 compact star clusters

(as mentioned above), 59 of them confirmed GCs. Clusters Id50552, Is50696, and Id50826 of Perelmuter et al. (1995) are numbers 87, 40, and 8 of Chandar et al. (2001), and objects 13 and 15 of Schroder et al. (2002) are 1 and 7 of Chandar et al. (2001), respectively. Altogether, there are 95 GCs, which are listed in Table 1 [col. (1) is the name of the GC, and cols. (2) and (3) are the *V*-band magnitude and $(B-V)_0$ color, respectively].

2.2. Reddening

In order to obtain intrinsic colors for the GCs, in addition to the absolute magnitudes, the photometric data should be corrected for reddening from the foreground extinction contribution of the Milky Way and for the internal reddening due to varying optical paths through the disk of M81. The total reddening in M81 (foreground plus M81 contribution) has been measured by a number of authors (e.g., Freedman et al. 1994; Kong et al. 2000). We only mention here that Kong et al. (2000) obtained the reddening maps of M81 based on the images in 13 intermediate-band filters from 3800 to 10000 Å. To determine the metallicity, age, and reddening distributions for M81, Kong et al. (2000) found the best match between the observed colors and the predictions from the single stellar population models of G. Bruzual & S. Charlot (1996, unpublished). A map of the interstellar reddening in a substantial portion of M81 were obtained. We used the reddening data of Kong et al. (2000). For a few clusters not presented in Kong et al. (2000) that fall near the edges of the images, we adopt the mean reddening value of 0.13. Since Chandar et al. (2001) also used the reddening data of Kong et al. to deredden their star clusters, we only deredden the GCs of Perelmuter et al. (1995) and Schroder et al. (2002). These local reddening values are listed in column (4) of Table 1. For completeness, we also list the reddening data for the GCs of Chandar et al. (2001).

3. PROPERTIES OF GLOBULAR CLUSTERS

3.1. Luminosity Function and Color-Magnitude Diagram

We show in Figure 1 the luminosity functions for all the sample GCs in M81. The magnitudes are corrected for extinction based on the local E_{B-V} value given in column (3) of Table 1 and the optical Galactic extinction law with $R_v = 3.1$ and a distance modulus for M81 of 27.8 (Freedman et al. 1994; Chandar et al. 2001). We can see that the M81 GC luminosity function is not unimodal (without an apparent peak). However, with a fainter completeness limit, the turnover may appear.

Figure 2 plots a $(B-V)_0$ versus M_V color-magnitude diagram for the M81 GCs. Colors have been dereddened by the local E_{B-V} value given in column (3) of Table 1. From Figure 2, we note that there are some GCs that have $(B-V)_0$ greater than 1.0. By comparison with the $(B-V)_0$ of Galactic GCs (Harris & Racine 1979) and M31 GCs (Barmby et al. 2000), these M81 GCs have high $(B-V)_0$. These red colors may result from enhanced foreground reddening, compared to the applied E_{B-V}. In particular, there is a GC (96 of Chandar et al. 2001) that has $(B-V)_0 = 1.778$, which is too high.

Figure 3 shows the $(B-V)_0$ histogram for our sample of globular clusters, and two color peaks clearly appear. Using deep F555W and F814W images from WFPC2 on board the *HST*, Kundu & Whitmore (2001) presented the results of the GC systems of 28 elliptical galaxies, in which the $V-I$ color distributions of at least 50% of the sample galaxies appear to be bimodal. In addition, from *HST* imaging in F555W and F814W filters, Larsen et al. (2001) studied the GCs in 17 relatively nearly early-type galaxies and found that a sum of two Gaussians provides a better fit to the observed color distribution than a single Gaussian. To make quantitative statements about the bimodality of $(B-V)_0$ in this paper, a KMM test (Ashman et al. 1994) is applied to the data. This test uses a maximum likelihood method to estimate the probability that the data distribution is better modeled as a sum of two Gaussians than as a single Gaussian. Here we use a homoscedastic test (i.e., the two Gaussians are assumed to have the same dispersion). The $(B-V)_0$ of the two peaks, the *P*-value, and the number of GCs assigned to each peak by the KMM test are $(B-V)_0 \approx 0.98$ and 0.66, 0.071, and 67 and 27, respectively. The *P*-value is in fact the probability that the data are drawn from a single Gaussian distribution. Since GC 96 of Chandar et al. (2001) has very high $(B-V)_0$ [$= 1.778$], we do not include it when conducting the KMM test. We note that the second Gaussian peak looks like a terrible fit, which may be because the data sample is not large enough. Barmby et al. (2000) analyzed the distribution of 10 intrinsic colors for the 221 M31 GCs and tested the color distributions of these GCs for bimodality using the KMM algorithm (Ashman et al. 1994); the peaks of the $(B-V)_0$ are 0.83 and 0.68. The peaks of the other intrinsic color distributions are presented in Table 8 of Barmby et al. (2000). For the color distributions of the Galactic GCs, Barmby et al. (2000) only plotted the distribution of $(V-I)_0$ and did not apply the KMM test. From Figure 14 of Barmby et al. (2000), two clear peaks in the distribution of $(V-I)_0$ can be seen.

3.2. Metallicity Distribution of the Sample Globular Clusters Using only Spectroscopic Data

Perelmuter et al. (1995) obtained the spectra for 25 M81 GCs with the Hydra multifiber positioner and bench spectrograph on the KPNO 4 m telescope. Schroder et al. (2002) then observed 16 M81 GCs with the Low Resolution Imaging Spectrograph on the Keck I telescope and presented the moderate-resolution spectroscopy for these GCs, in addition to the metallicities for 15 of the 16 GCs. There is one GC, number 12 of Schroder et al. (2002), for which the metallicity was not obtained, since a transient phenomenon was occurring in this GC at the time of the observation. Thus, there are a total of 40 GCs for which we have metallicities, which are listed in Table 2. However, some of the Perelmuter et al. (1995) sample GC metallicities have large uncertainties, which can create un-

TABLE 1
GLOBULAR CLUSTER SAMPLE AND PROPERTIES

ID[a] (1)	V (mag) (2)	$B-V$ (mag) (3)	E_{B-V} (mag) (4)	ID[a] (1)	V (mag) (2)	$B-V$ (mag) (3)	E_{B-V} (mag) (4)
Id30244	19.76	0.77	0.130	CFT31	22.086 ± 0.053	1.231 ± 0.208	0.180
Is40083	18.39	0.69	0.130	CFT32	20.478 ± 0.018	1.372 ± 0.085	0.130
Is40165	18.23	0.69	0.130	CFT34	21.029 ± 0.023	0.906 ± 0.072	0.150
Is40181	18.93	1.09	0.130	CFT37	19.882 ± 0.009	0.661 ± 0.013	0.130
Is50037	18.04	0.55	0.130	CFT38	19.835 ± 0.006	0.808 ± 0.012	0.130
Is50225	18.43	0.97	0.026	CFT39	19.319 ± 0.005	0.832 ± 0.009	0.090
Is50233	19.18	0.89	0.125	CFT40	18.298 ± 0.002	0.581 ± 0.004	0.080
Is50286	20.16	0.89	0.216	CFT41	19.721 ± 0.006	0.696 ± 0.009	0.080
Id50357	19.67	1.27	0.130	CFT42	20.033 ± 0.011	0.717 ± 0.014	0.070
Is50394	19.24	0.57	0.195	CFT43	21.657 ± 0.048	0.675 ± 0.057	0.070
Id50401	19.93	1.22	0.242	CFT44	21.325 ± 0.027	0.706 ± 0.051	0.100
Id50415	19.24	0.85	0.237	CFT45	20.534 ± 0.015	0.709 ± 0.018	0.110
Id50785	19.08	0.86	0.238	CFT46	20.905 ± 0.016	0.689 ± 0.021	0.100
Is50861	19.69	0.88	0.175	CFT49	21.911 ± 0.054	0.702 ± 0.079	0.120
Is50886	18.06	0.91	0.067	CFT51	20.681 ± 0.014	1.231 ± 0.035	0.100
Id50960	18.49	0.86	0.102	CFT53	20.947 ± 0.016	0.653 ± 0.024	0.130
Is51027	19.36	0.55	0.130	CFT56	20.259 ± 0.010	0.710 ± 0.014	0.110
Is60045	18.70	0.80	0.130	CFT58	23.065 ± 0.090	1.511 ± 0.142	0.150
Id70319	20.77	0.99	0.130	CFT62	19.051 ± 0.004	0.915 ± 0.007	0.100
Id70349	20.12	0.91	0.130	CFT63	21.230 ± 0.026	0.654 ± 0.260	0.080
Is80172	18.97	0.91	0.130	CFT65	20.668 ± 0.027	0.622 ± 0.033	0.120
Is90103	18.01	0.60	0.130	CFT66	20.133 ± 0.017	0.627 ± 0.032	0.120
SBKHP1	18.54	1.10	0.100	CFT67	21.209 ± 0.035	0.842 ± 0.038	0.110
SBKHP2	18.97	1.02	0.066	CFT68	21.070 ± 0.020	0.704 ± 0.025	0.100
SBKHP3	18.35	1.04	0.114	CFT74	21.038 ± 0.019	0.652 ± 0.025	0.090
SBKHP4	19.24	1.05	0.057	CFT75	20.514 ± 0.011	0.795 ± 0.019	0.200
SBKHP5	18.45	1.04	0.065	CFT76	20.890 ± 0.014	0.599 ± 0.019	0.100
SBKHP6	18.80	0.97	0.077	CFT80	22.521 ± 0.036	0.653 ± 0.063	0.120
SBKHP7	19.05	1.00	0.082	CFT83	23.686 ± 0.061	0.698 ± 0.117	0.100
SBKHP8	18.01	1.04	0.075	CFT85	23.532 ± 0.046	0.708 ± 0.084	0.100
SBKHP9	18.76	0.98	0.089	CFT87	19.787 ± 0.008	1.132 ± 0.036	0.130
SBKHP10	20.08	0.84	0.146	CFT90	23.307 ± 0.106	1.315 ± 0.718	0.250
SBKHP11	18.59	0.82	0.063	CFT96	22.517 ± 0.047	1.778 ± 0.328	0.110
SBKHP12	18.70	1.00	0.166	CFT97	19.980 ± 0.008	0.870 ± 0.023	0.100
SBKHP14	19.03	0.92	0.084	CFT101	22.627 ± 0.132	0.779 ± 0.160	0.100
SBKHP16	18.73	0.99	0.144	CFT102	21.015 ± 0.027	1.379 ± 0.273	0.100
CFT1	19.170 ± 0.006	0.884 ± 0.020	0.180	CFT103	21.703 ± 0.035	0.723 ± 0.109	0.130
CFT5	19.826 ± 0.008	1.184 ± 0.029	0.270	CFT104	20.205 ± 0.012	0.865 ± 0.034	0.130
CFT6	20.263 ± 0.010	0.813 ± 0.035	0.120	CFT105	19.867 ± 0.011	0.953 ± 0.031	0.100
CFT7	18.785 ± 0.004	0.973 ± 0.015	0.090	CFT106	20.596 ± 0.027	0.968 ± 0.061	0.080
CFT8	20.191 ± 0.008	1.030 ± 0.025	0.130	CFT108	20.544 ± 0.027	0.980 ± 0.051	0.120
CFT15	22.462 ± 0.065	0.584 ± 0.130	0.060	CFT109	21.274 ± 0.056	1.178 ± 0.097	0.110
CFT16	22.258 ± 0.056	0.731 ± 0.149	0.090	CFT110	21.328 ± 0.075	0.842 ± 0.089	0.100
CFT20	21.340 ± 0.026	0.790 ± 0.085	0.120	CFT111	21.011 ± 0.031	0.901 ± 0.062	0.100
CFT21	21.860 ± 0.034	0.793 ± 0.109	0.140	CFT112	22.236 ± 0.111	0.643 ± 0.106	0.110
CFT22	20.668 ± 0.020	1.095 ± 0.105	0.110	CFT113	20.192 ± 0.014	1.065 ± 0.058	0.070
CFT28	23.688 ± 0.131	0.870 ± 0.163	0.110	CFT114	20.262 ± 0.020	0.658 ± 0.066	0.100
CFT30	20.649 ± 0.015	1.094 ± 0.053	0.270				

[a] SBKHP identifications are from Schroder et al. (2002); CFT identifications are from Chandar et al. (2001); the others are from Perelmuter et al. (1995).

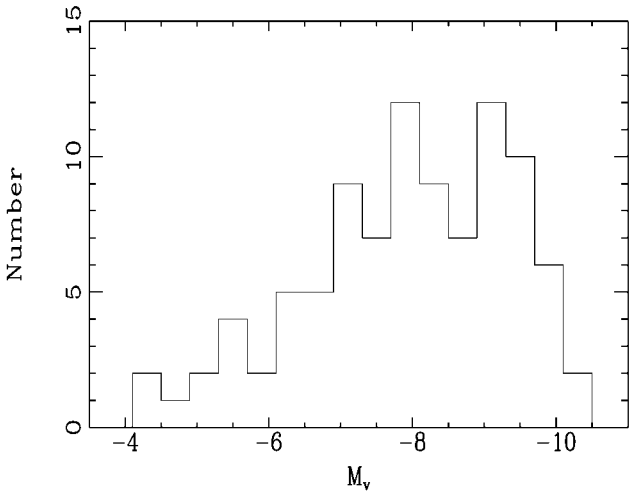

FIG. 1.—Luminosity function of the sample GCs.

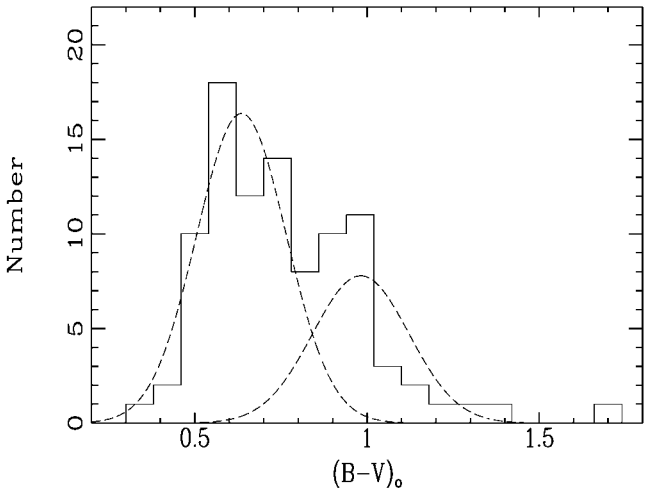

FIG. 3.—Color histogram distribution of the GC sample.

certainties in the metallicity distributions. Therefore, Figure 4 only shows the metallicity of 26 M81 GCs with metallicity uncertainties smaller than 1.0 dex. Figure 4 does not show two peaks, and perhaps because the number of sample GCs is too small. In order to enlarge the number of GCs, we use metallicities estimated from colors by the color-metallicity relation.

3.3. Color-Metallicity Correlation

Originally, Brodie & Huchra (1990) derived a correlation between the IR colors and metallicity of 23 low-reddening Galactic GCs. Kissler-Patig et al. (1998) studied the GCs of NGC 1399 using moderate-resolution, high signal-to-noise ratio spectroscopy and found that $V - I$ and metallicity are well correlated. To determine the reddening and use the color to predict metallicity, Barmby et al. (2000) performed linear regressions of the color-metallicity relation for M31 and Galactic GCs.

We present below the relation between intrinsic color in the B and V bands and metallicity for 26 M81 GCs for which we have spectroscopic metallicities that are smaller than 1.0 dex. We do an ordinary least-squares fit:

$$[\mathrm{Fe/H}] = a(B - V)_0 + b. \quad (1)$$

Figure 5 shows this fit. The fit results are $a = 2.41 \pm 0.46$, $b = -3.08 \pm 0.37$, and the linear correlation coefficient $r = 0.73$.

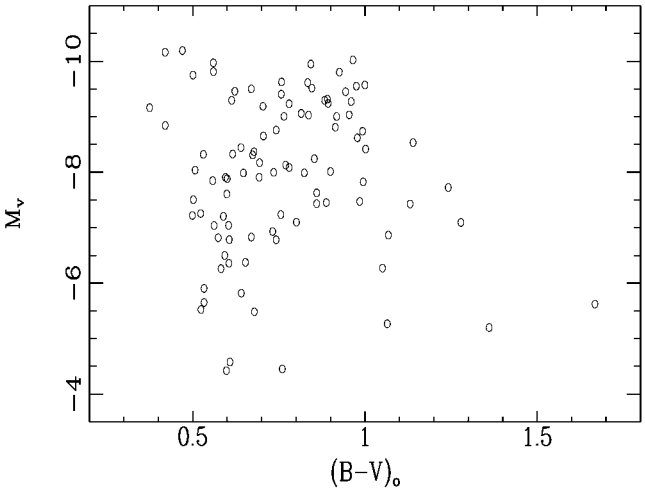

FIG. 2.—Color-magnitude diagram of the GC sample.

TABLE 2
METALLICITIES FOR SOME SAMPLE GLOBULAR CLUSTERS

ID	[Fe/H]	ID	[Fe/H]
Id30244	−1.76 ± 1.78	Is60045	−1.03 ± 0.97
Is40083	−1.29 ± 0.80	Id70319	−2.31 ± 1.69
Is40165	−1.57 ± 0.43	Id70349	−2.41 ± 1.15
Is40181	0.64 ± 1.43	Is80172	−0.77 ± 0.68
Is50037	−2.34 ± 0.83	Is90103	−2.23 ± 0.99
Is50225	−0.04 ± 0.59	SBKHP1	−1.207 ± 0.369
Is50233	−1.75 ± 1.02	SBKHP2	−0.707 ± 0.167
Is50286	−0.04 ± 1.85	SBKHP3	−0.211 ± 0.193
Id50357	−3.62 ± 2.97	SBKHP4	−0.407 ± 0.088
Is50394	−1.50 ± 1.29	SBKHP5	−1.086 ± 0.091
Id50401	−0.04 ± 1.00	SBKHP6	−1.493 ± 0.206
Id50415	−1.90 ± 0.71	SBKHP7	−0.955 ± 0.098
Id50552	0.98 ± 2.04	SBKHP8	−0.698 ± 0.058
Is50696	−1.86 ± 0.50	SBKHP9	−1.212 ± 0.133
Id50785	−0.72 ± 1.17	SBKHP10	−1.322 ± 0.356
Id50826	−1.46 ± 1.11	SBKHP11	−1.114 ± 0.409
Is50861	−1.71 ± 1.00	SBKHP13	−1.055 ± 0.062
Is50886	−1.79 ± 0.87	SBKHP14	−1.107 ± 0.074
Id50960	−1.79 ± 0.64	SBKHP15	−1.014 ± 0.713
Is51027	−2.47 ± 1.01	SBKHP16	−0.674 ± 0.044

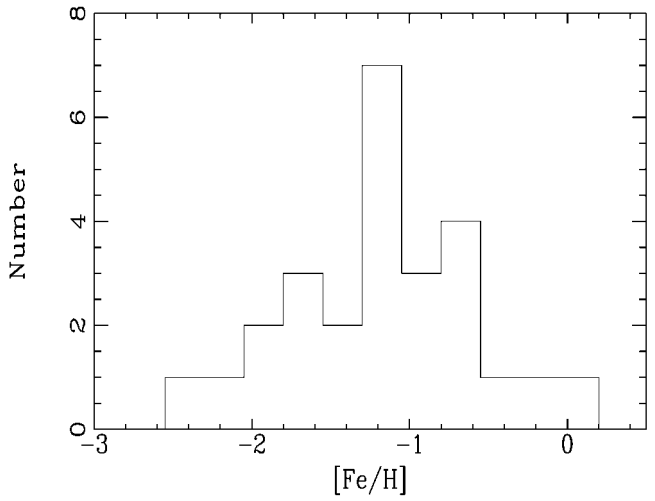

FIG. 4.—Metallicity diagram for the GCs that only have spectroscopic data.

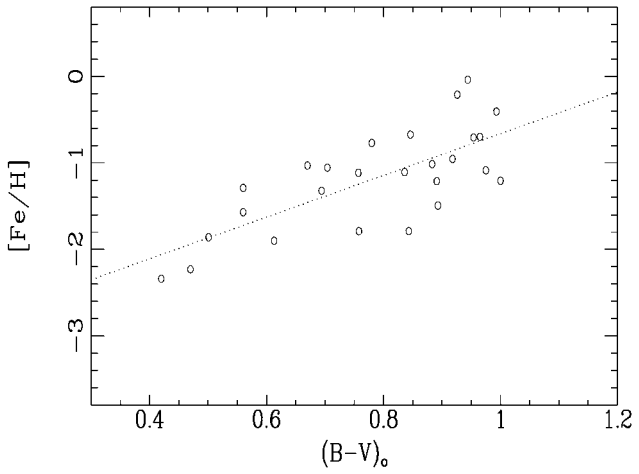

FIG. 5.—Color in *BV* bands vs. spectroscopic metallicities for M81 GCs.

Couture et al. (1990) established the intrinsic $B - V$ color-metallicity relation for 65 Galactic GCs, using the data from Reed et al. (1988) and Zinn (1985), for which the foreground reddening is low ($E_{B-V} \leq 0.4$). The relation is reasonably well known:

$$(B - V)_0 = 0.200[\mathrm{Fe/H}] + 0.971. \quad (2)$$

Barmby et al. (2000) also presented the intrinsic $B - V$ color-metallicity relation for 88 Galactic GCs with $E_{B-V} < 0.5$ (the database of Galactic GC parameters were from the 1999 June version of Harris [1996]):

$$(B - V)_0 = 0.159 \pm 0.011[\mathrm{Fe/H}] + 0.92 \pm 0.02. \quad (3)$$

In order to make comparisons with the intrinsic $B - V$ color-metallicity relation for the Galactic GCs, we establish this relation using the data from the 26 M81 GCs used in Figure 5:

$$(B - V)_0 = 0.222 \pm 0.042[\mathrm{Fe/H}] + 1.05 \pm 0.05. \quad (4)$$

We can see that the intrinsic $B - V$ color-metallicity relation between the Galactic GCs and the M81 GCs is consistent by comparing equations (2), (3), and (4).

3.4. Metallicity Distribution of All the Sample Globular Clusters

We use the above color-metallicity correlation to derive metallicities for the sample GCs that do not have spectroscopic metallicities or that have metallicity uncertainties larger than 1 dex. We plot metallicity distribution in Figure 6, including the metallicities derived using the above color-metallicity correlation. To make quantitative statements about bimodality, we also apply a KMM test (Ashman et al. 1994) to the data. The metallicities of the two peaks, the *P*-value, and the numbers of clusters assigned to each peak by the KMM test are [Fe/H] ≈ -1.45 and -0.54, 0.024, and 74 and 20, respectively. Since the GC 96 of Chandar et al. (2001) has very high $(B - V)_0$ [$(B - V)_0 = 1.778$] and the metallicity obtained using the color-metallicity correlation is too rich (0.95 dex), we do not include it when performing the KMM test.

4. SUMMARY AND DISCUSSION

In this paper, we present catalogs of photometric and spectroscopic data and statistical correlations for M81 GCs. Using the KMM test, we find that the distribution of intrinsic *B* and *V* colors and metallicities are bimodal. The correlation between spectroscopic metallicity and intrinsic *B* and *V* color also exists as it does for the Milky Way and M31.

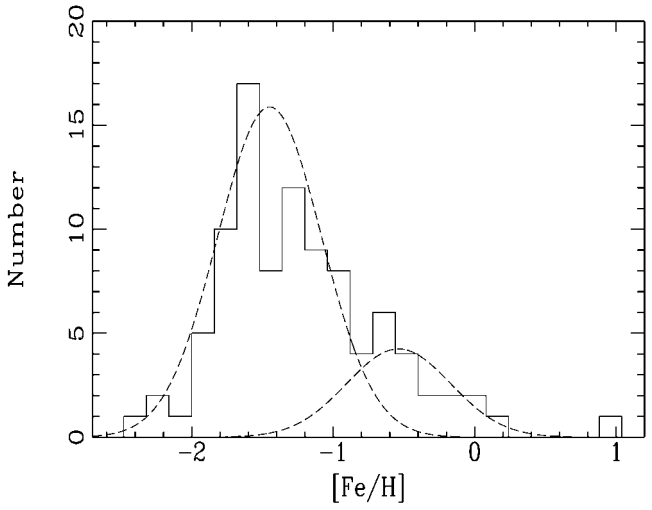

FIG. 6.—Metallicity diagram for all GCs.

We would like to thank the anonymous referee for his/her insightful comments and suggestions that greatly improved this paper. This work has been supported by the Chinese National Key Basic Research Science Foundation (NKBRSF TG199075402) and in part by the Chinese National Science Foundation (number 10473012).

REFERENCES

Ashman, K. A., Bird, C. M., & Zepf, S. E. 1994, AJ, 108, 2348
Barmby, P., Huchra, J., Brodie, J., Forbes, D., Schroder, L., & Grillmair, C. 2000, AJ, 119, 727
Brodie, J. P., & Huchra, J. P. 1990, ApJ, 362, 503
Chandar, R., Ford, H. C., & Tsvetanov, Z. 2001, AJ, 122, 1330
Côté, P. 1999, AJ, 118, 406
Couture, J., Harris, W. E., & Allwright, J. W. B. 1990, ApJS, 73, 671
Freedman, W. L., Wilson, C. D., & Madore, B. F. 1994, ApJ, 427, 628
Harris, W. E., & Racine, R. 1979, ARA&A, 17, 241
Harris, W. H. 1996, AJ, 112, 1487
Kissler-Patig, M., Brodie, J. P., Schroder, L. L., Forbes, D. A., Grillmair, C. J., & Huchra, J. P. 1998, AJ, 115, 105
Kong, X., et al. 2000, AJ, 119, 2745
Kundu, A., & Whitmore, B. C. 2001, AJ, 121, 2950
Larsen, S. S., et al. 2001, AJ, 121, 2974
Perelmuter, J. M., Brodie, J. P., & Huchra, J. 1995, AJ, 110, 620
Perelmuter, J. M., & Racine, R. 1995, AJ, 109, 1055
Perrett, K. M.. et al. 2002, AJ, 123, 2490
Reed, B. C., Hesser, J. E., & Shawl, S. J. 1988, PASP, 100, 545
Schroder, L. L., Brodie, J. P., Kissler-Patig, M., Huchra, J. P., & Phillips, A. C. 2002, AJ, 123, 2473
West, M. J., Côté, P., Marzke, R. O., & Jordan, A. 2004, Nature, 427, 31
Zepf, S. E., & Ashman, K. A. 1993, MNRAS, 264, 611
Zinn, R. 1985, ApJ, 293, 424